

SOLAQUA: SINTEF Ocean Large Aquaculture Robotics Dataset

Sveinung Johan Ohrem^{1,†}, Bent Haugaløkken¹, Eleni Kelasidi^{1,2}

¹ Department of Aquaculture, SINTEF Ocean, Trondheim, Norway

² Department of Mechanical and Industrial Engineering, NTNU, Trondheim, Norway

[†] Corresponding author: sveinung.ohrem@sintef.no

Abstract—This paper presents a dataset gathered with an underwater robot in a sea-based aquaculture setting. Data was gathered from an operational fish farm and includes data from sensors such as the Waterlinked A50 DVL, the Nortek Nucleus 1000 DVL, Sonardyne Micro Ranger 2 USBL, Sonoptix Multibeam Sonar, mono and stereo cameras, and vehicle sensor data such as power usage, IMU, pressure, temperature, and more. Data acquisition is performed during both manual and autonomous traversal of the net pen structure. The collected vision data is of undamaged nets with some fish and marine growth presence, and it is expected that both the research community and the aquaculture industry will benefit greatly from the utilization of the proposed SOLAQUA dataset.

I. INTRODUCTION

Aquaculture is and will be an important contributor to the production of protein and food in the years to come. Aquaculture as an industry is found all over the world, with varying production methods dominating depending on the country [1]. In Norway, sea-based aquaculture is the current industry standard, as the Norwegian geography with sheltered fjords invites this production type. Atlantic salmon (*salmo salar*) is the most commonly farmed species and the production method of choice is net pens. These net pens, and the surrounding infrastructure, are in constant need of inspection, maintenance and repair (IMR) operations. The aquaculture industry in Norway has adapted underwater remotely operated vehicles (ROVs) for majority of the inspection and intervention tasks in fish farms.

Typical ROV operations in aquaculture range from net and mooring inspections and cleaning, to fish monitoring and net pen installations [2].

A net pen offers a unique domain for underwater robots: The operations are normally performed in - or close to - the splash zone with currents and waves affecting the robot's states. The environment is dynamic, with large moving structures and several potentially moving obstacles. There are hundreds of thousands of fish in a net pen which will interfere sensor signals and block camera views. All of this combined with the risks and costs of performing sea-based operations makes aquaculture a challenging domain for underwater robotics which is likely to benefit greatly from the development of higher levels of autonomy [2].

Research efforts have been made over the last years to advance the level of autonomy in the mentioned areas as these operations are mostly manually performed today [3].

Early results include novel methods for navigation in net pens using a Doppler velocity logger (DVL) and ultra-short baseline (USBL) system [4]. This work led to the development of a net-following algorithm [5] which has been demonstrated in several later works, e.g., [6]–[8]. Navigation using low-cost sensor systems was investigated in [9] where various low-cost sonar and DVL technologies are shown to be suitable for navigation purposes in net pens. Camera-based methods are investigated, for example, in [10], [11] with the goal of reducing the number of navigation sensors needed on underwater vehicles in aquaculture.



(a) ROV with sensor configuration 1. (b) ROV with sensor configuration 2.

Fig. 1: ROV with two different sensor configurations.

As methods driven by artificial intelligence (AI) and machine learning (ML) are adapted in the aquaculture robotics domain, the need for datasets to train AI and ML models is of great importance to contribute and advance the research on robust methods for fully autonomous IMR operations, and thus address current and future challenges of the aquaculture industry. Particularly in the field of vision-based and multi-modal navigation, where camera images paired with e.g., position measurements from other sensors such as DVL and USBL can have significant value.

To this end, we present the SINTEF Ocean Large Aquaculture Dataset, SOLAQUA, consisting of navigation sensor data, sonar images, mono and stereo camera images, and vehicle data, all captured in a fully operational fish farm. The dataset was captured while performing manual control of a remotely operated vehicle (BlueROV2) as well as during autonomous traversal of the net structure using the previously developed net following algorithm. The data may be utilized

TABLE I: BlueROV2 Technical Specifications

Feature	Description
Size (L x W x H) (Config 1)	457 x 436 x 397 [mm]
Size (L x W x H) (Config 2)	457 x 436 x 541 [mm]
Weight in air/water (Config 1)	15/0 [kg]
Weight in air/water (Config 2)	18/0 [kg]
Number of thrusters	8
Communication	Ethernet, UDP
Degrees of Freedom	6
Power	Battery, 14.8 [V]

for the development of navigation methods, developing novel computer vision techniques for navigation and inspection, simulation purposes, to verify novel control methods, and much more. Examples of use of the dataset for development of robust localization and mapping methods for UUVs operating in industrial scale fish farms can be found in e.g., [12].

Several dedicated campaigns of field trials in October 2023 and in August 2024 have been performed to collect data from two different industrial-scale fish farms. During these trials, the ROV operated inside the net pen under diverse environmental conditions while performing net inspection of nets with different net grid size. The dataset consists of numerous subsets from ROV operating in different depths with various speeds, keeping different net-relative distances from the net pen, and facing different environmental conditions lasting between 1 and 2 minutes. The ROV faces the net structure during the runs, hence images are of undamaged nets with some marine growth. Some fish are present, but the purpose of this dataset is not to capture images of fish. To our knowledge, no similar dataset exist.

This paper briefly describes the platform used for gathering the data (a BlueROV2) and the data acquisition procedure. In addition, information are presented to give detailed overview of the sensors, their logging frequency and position on the ROV. This overview together with the concrete examples of data found in the dataset can be utilized from the research community to develop and propose novel methods.

The dataset can be found at the following website: <https://data.sintef.no/feature/fe-a8f86232-5107-495e-a3dd-a86460eebef6> and is under CC BY-SA license.

II. MULTI-MODAL UNDERWATER PLATFORM FOR DATA COLLECTION AND AUTONOMOUS OPERATIONS

In the presented dataset the vehicle was either moved manually or autonomously using net following. Net following refers to an automatic control procedure where the vehicle moves relative to the net at a desired distance, heading angle, and velocity relative to the net structure [5]. All datasets are logged with time-synchronization using ROS (Robot Operating System) as .bag-files.

As shown in Table I and Figure 1 two configurations of the BlueROV2 was used to gather the datasets. Each configuration results in a vehicle with different dimensions and weights, and with a variety of integrated relevant sensors.

A. Sensors

A list of sensors used to gather the datasets is shown in Table IV. Note that some custom ROS messages have been used. These can be downloaded alongside the respective datasets. Frequency values may sometimes vary slightly throughout a test (denoted with a \sim symbol). For acoustic sensors, the frequency may vary depending on the distance between the sensor and the target object. For camera data, datasets contain either Image or CompressedImage (ROS) message types, where more recent trials have chosen to use CompressedImage to reduce data size.

TABLE II: Overview of performed tests

Purpose of test	Number of datasets
Camera Calibration (CC)	3
Manual Control (MC)	6
Net following horizontal (NFH)	54

B. Sensors and sensor placements for different vehicle configurations

1) *Sensor placement*: The sensor placements are given relative to the vehicle’s IMU, and is given in the vehicle’s BODY-frame. The electronics enclosure (4”), which houses the main electronics including the camera and the IMU, has a length of 0.3 meters (which can be used in case you wish to use the center of origin (CO) as your origin). Sensor placements are given in Table V.

C. Camera calibration parameters

Matlab (R2022b) and the in-built camera calibration apps Camera Calibrator and Stereo Camera Calibrator have been used to obtain the camera parameters (intrinsic, extrinsic). In the calibration procedure, images were collected by recording a video containing a checkerboard at various locations within the video frames. The procedure for performing the calibration can be found in the documentation of the camera calibration apps. The parameters for the mono and stereo camera systems can be found in Table III and Table VI, respectively. Distances are given in millimeters.

In general, obtaining absolute ground truth measurements in underwater environments is challenging. To address this challenge and obtain ground truth distances to the net, passive visual markers (i.e. AprilTags) have been placed directly on the net surface during field trials, see Figure. 10.

III. DATASETS

Datasets contain tests that may be associated with two log-files, one for video/images (including sonar data), and

TABLE III: Mono camera parameters

Camera matrix	$\begin{bmatrix} 348.5190 & 0 & 317.4431 \\ 0 & 349.9505 & 168.9469 \\ 0 & 0 & 1.0000 \end{bmatrix}$
Reprojection error	0.191835
Distortion coefficients	[0.0117, 0.0300, -0.0328, 0, 0]

TABLE IV: Sensor Specifications and ROS Topics

Sensor	Frequency	Additional info	ROS topic	ROS Message name
IMU	~ 15 – 25Hz ~ 15 – 25Hz	Acc, Gyro Θ (includes the IMU’s internal estimates of roll, pitch and yaw)	/sensor/imu /sensor/attitude*	IMU Attitude
Barometer	<10 Hz	Pressure, depth, temperature	/sensor/depth_temperature	DepthTemperature
Ping Echosounder	~ 10Hz	Includes distance and confidence on measurement	/sensor/ping	Ping
Ping360	<25 Hz	Logged “range” data is experimental and may be inaccurate in trials from 2023-2024	/sensor/ping360	Ping360
DVL DVL-A50	~ 10 Hz	-	/sensor/dvl_position, /sensor/dvl_velocity	DVLPosition DVLBeam, DVLVelocity
DVL Nucleus1000	1-8 Hz	-	/nucleus1000dvl/bottomtrack	Nucleus1000_bottomtrack
	100 Hz	-	/nucleus1000dvl/imu	Nucleus1000_imu
	10 Hz	-	/nucleus1000dvl/ins	Nucleus1000_ins
	50 Hz	-	/nucleus1000dvl/magnetometer	Nucleus1000_magnetometer
USBL: MicroRanger 2	0.5-2 Hz	-	/sensor/usbl	SonardyneUSBL2
Multi-beam sonar: Sonoptix Echo	<25 Hz	-	/sensor/sonoptix_echo/image	SonoptixECHO
Camera	15/25 FPS	RGB, 1080p / 720p	/bluerov2/image /image/compressed_image/data	sensor_msgs/Image sensor_msgs/CompressedImage
Stereo camera	15/25 FPS	RGB, 1080p / 720p	-	sensor_msgs/Image sensor_msgs/CompressedImage sensor_msgs/Image sensor_msgs/CompressedImage

TABLE V: Sensor Configurations

Sensor	Configuration 1	Configuration 2
IMU	[0, 0, 0, 0, 0, 0]	(See Configuration 1)
Barometer	[-0.21, 0, 0, 0, 0, 0]	(See Configuration 1)
Ping Echosounder	[0.05, -0.06, 0.13, 0, 0, 0]	N/A
Ping360	[0.07, -0.08, -0.16, 0, 0, -180.0]	(See Configuration 1)
DVL DVL-A50	[0.10, 0.04, 0.13, -90, 0, -90]	(See Configuration 1)
DVL Nucleus1000	N/A	[0.10, 0.04, 0.11, -90, 0, -90]
USBL	[0.08, 0.24, -0.15, 0, 0, 0]	(See Configuration 1)
Multi-beam sonar	N/A	[0.09, 0.04, -0.11, 0, 5, 0]
Camera	[0.09, 0.04, 0, 0, 0, 0]	(See Configuration 1)
Stereo camera (L)	[0.04, 0.095, 0.26, 0, 0, 0]	(See Configuration 1)
Stereo camera (R)	[0.04, -0.015, 0.26, 0, 0, 0]	(See Configuration 1)

TABLE VI: Stereo camera parameters

Translation (baseline)	[-110.16, 0.14, 0.65]									
Mean Reprojection Error	0.4170									
Fundamental matrix	<table border="1"> <tr> <td>-0.0000</td> <td>0.0000</td> <td>-0.0016</td> </tr> <tr> <td>-0.0000</td> <td>-0.0000</td> <td>0.1363</td> </tr> <tr> <td>0.0004</td> <td>-0.1364</td> <td>0.5083</td> </tr> </table>	-0.0000	0.0000	-0.0016	-0.0000	-0.0000	0.1363	0.0004	-0.1364	0.5083
-0.0000	0.0000	-0.0016								
-0.0000	-0.0000	0.1363								
0.0004	-0.1364	0.5083								
Essential matrix	<table border="1"> <tr> <td>-0.0009</td> <td>3.4838</td> <td>0.0517</td> </tr> <tr> <td>-0.8839</td> <td>-1.2784</td> <td>110.2245</td> </tr> <tr> <td>0.0252</td> <td>-110.1729</td> <td>-1.2772</td> </tr> </table>	-0.0009	3.4838	0.0517	-0.8839	-1.2784	110.2245	0.0252	-110.1729	-1.2772
-0.0009	3.4838	0.0517								
-0.8839	-1.2784	110.2245								
0.0252	-110.1729	-1.2772								
CAMERA1 Focal Length	[884.1997, 823.9808]									
CAMERA1 Principal Point	[637.8639, 354.3048]									
CAMERA1 Radial Distortion	[0.2474, 0.3499]									
CAMERA1 Tangential Distortion	[0, 0]									
CAMERA1 Skew	0									
CAMERA1 Camera matrix	<table border="1"> <tr> <td>884.1997</td> <td>0</td> <td>637.8639</td> </tr> <tr> <td>0</td> <td>823.9808</td> <td>354.3048</td> </tr> <tr> <td>0</td> <td>0</td> <td>1.0000</td> </tr> </table>	884.1997	0	637.8639	0	823.9808	354.3048	0	0	1.0000
884.1997	0	637.8639								
0	823.9808	354.3048								
0	0	1.0000								
CAMERA2 Focal Length	[877.3510, 817.2770]									
CAMERA2 Principal Point	[691.8459, 342.6457]									
CAMERA2 Radial Distortion	[0.2532, 0.2153]									
CAMERA2 Tangential Distortion	[0, 0]									
CAMERA2 Skew	0									
CAMERA2 Camera matrix	<table border="1"> <tr> <td>877.3510</td> <td>0</td> <td>691.8459</td> </tr> <tr> <td>0</td> <td>817.2770</td> <td>342.6457</td> </tr> <tr> <td>0</td> <td>0</td> <td>1.0000</td> </tr> </table>	877.3510	0	691.8459	0	817.2770	342.6457	0	0	1.0000
877.3510	0	691.8459								
0	817.2770	342.6457								
0	0	1.0000								

one for all other data, denoted "timestamp"_video.bag and "timestamp"_data.bag, respectively.

A. Data gathering procedures and methods

The data was gathered using a BlueROV2 vehicle. Each run was performed using either manual control or autonomous net following. Some runs were also performed solely to gather data for stereo camera calibration. The path driven during the runs was more or less the same for every run, but the depth, speed and distance to the net may vary both during the runs and between runs. See details on the dataset website.

In the dataset you may find the following abbreviations: Manual Control (MC), Net-following (NF), Net-following horizontal (NFH), and Camera Calibration (CC). The dataset was recorded in August 2024. The number of datasets for each performed test are presented in Table II.

1) *Manual control*: Logging of data started when the vehicle was at the desired depth and distance to the net. The pilot used the *depth hold* mode of the BlueROV2, i.e., the depth and the angles (roll, pitch, yaw) are automatically controlled. The pilot attempted to perform a net following maneuver, i.e., maintaining a certain distance to the net while moving sideways.

2) *Autonomous net following*: Logging of data started when the vehicle was at the desired depth and at a certain distance from the net not too far from the initial desired distance. The net following was then performed, i.e., the vehicle was automatically commanded to move sideways with a certain speed, distance and heading relative to the net. The speed of the ROV was controlled using the adaptive controller from [13]. The depth was controlled by a decoupled depth controller.

IV. EXAMPLE DATA

In this section, examples of some of the collected data from the datasets will be presented (Figures 2 - Figure 11). Figure 2 shows data from the Water Linked A50 DVL, the Nortek Nucleus 1000 DVL, and the desired speed of the ROV during one particular trial. Note that any deviation from the desired speed is not an indicator of sensor performance. Both sensors experience instances of invalid data points. These points are replaced by the latest valid data point for plotting purposes.

In addition to the raw measurements, using the DVL beam measurements from Water Linked A50 DVL and adapting the method developed in [5], the dataset includes estimations of the net-relative distance, net-relative heading and net-relative speed for each performed trials. Figures 3, Figure 4 and Figure 5 show the net-relative distance, net-relative heading and net-relative speed for another trial, respectively.

The global position of the ROV is obtained using the Sonardyne MicroRanger 2 USBL during these trials. Figure 6 shows the ROV position in the North-East frame as captured by this system. From this it is possible to see that the ROV is following the curved shape of the net pen structure.

Although the sonar images are best viewed as a video stream, Figure 7 shows one image from the Sonoptix Multi-beam sonar containing the net structure and some fish. Figure 8

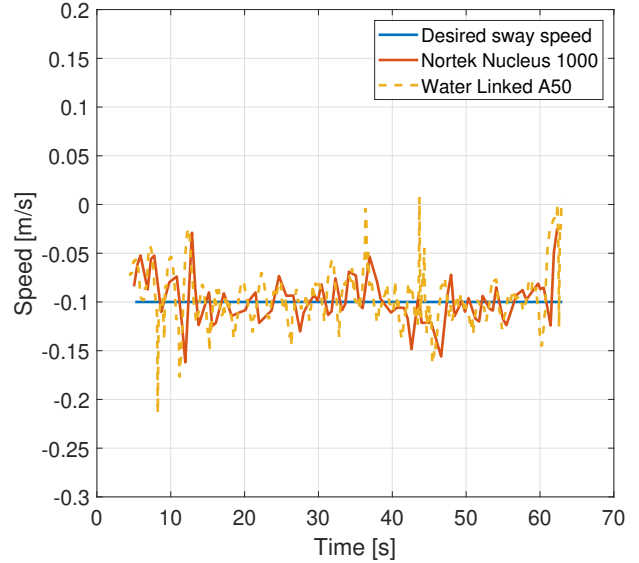


Fig. 2: The net-relative sway speed measured by the Water Linked A50 and the Nortek Nucleus 1000 DVL.

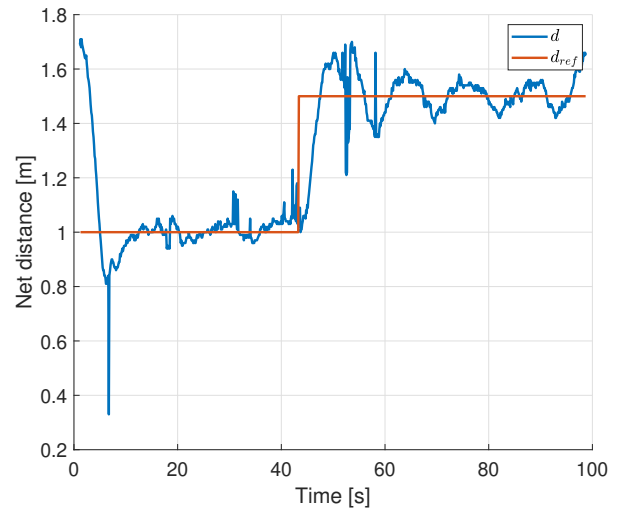


Fig. 3: ROV distance to net (blue) and desired distance (red).

shows a screenshot of data from the Ping360 sensor. The net and some fish are present. Lastly, Figure 9, Figure 10, and Figure 11 show screenshots from the mono and stereo cameras, respectively.

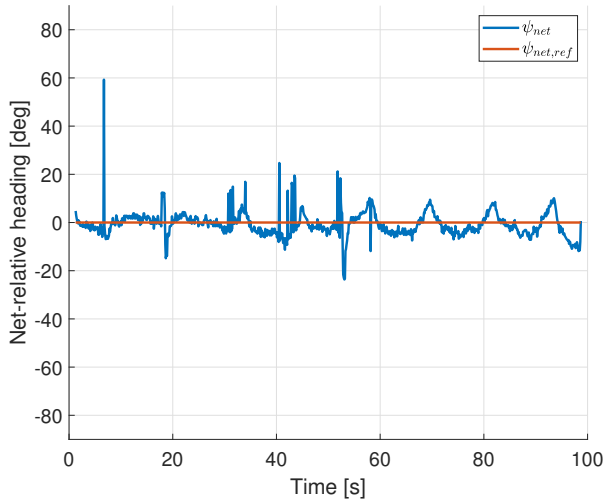


Fig. 4: ROV heading relative to net (blue) and desired net relative heading (red).

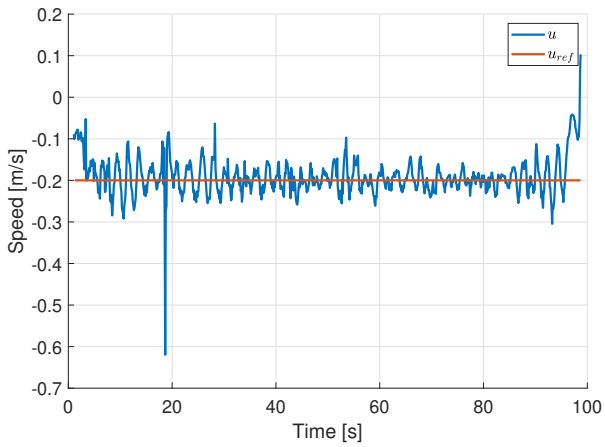


Fig. 5: ROV net relative sway speed (blue) and desired speed (red).

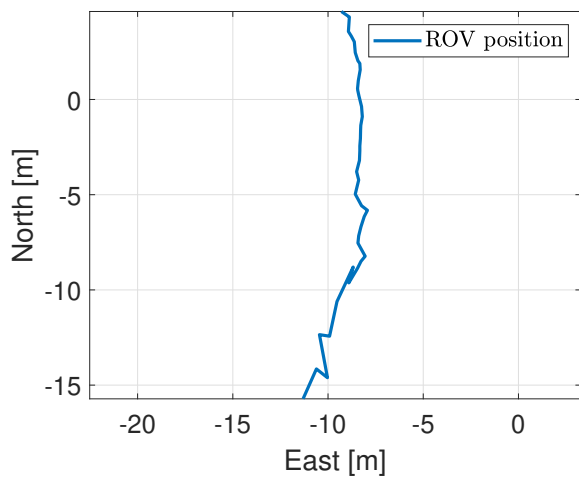


Fig. 6: ROV position in the North-East frame.

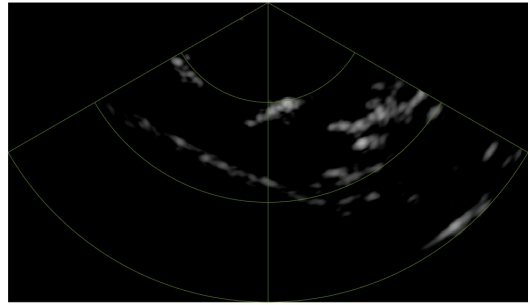


Fig. 7: Image from the Sonoptix Multibeam sonar.

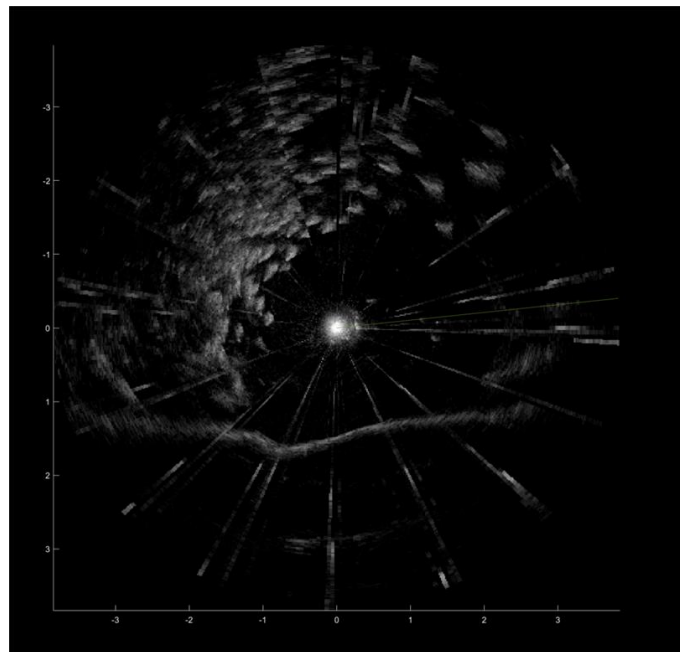


Fig. 8: The data from the Ping360 sensor.



Fig. 9: Screenshot from the mono camera during a trial.

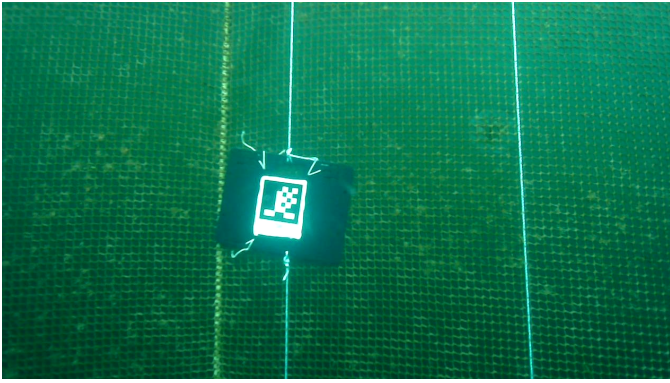


Fig. 10: Screenshot from the mono camera showing the AprilTag

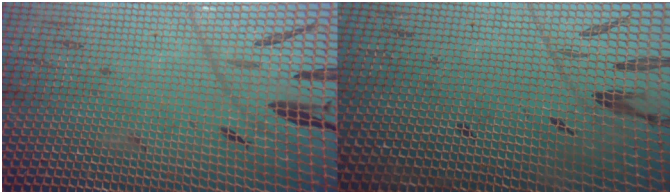


Fig. 11: Screenshot from the stereo camera during a trial.

V. CONCLUSIONS

In this paper, we have presented a new large dataset, SOLAQUA, acquired during both manual and autonomous net following ROV operations in industrial scale fish farms in Norway. The proposed dataset contains data from the most commonly used acoustic and vision sensors in underwater domain. The released dataset covers a diverse set of software-synchronized measurements, including undamaged nets with some fish and marine growth presence. The datasets consists of numerous subsets from ROV operating in different depths with various speeds, keeping different net-relative distances from the net pen, and facing diverse environmental conditions. Our dataset will not only contribute to facilitate research on resilient underwater perception and robust navigation autonomy of underwater robotic systems operating in dynamic environments, but also provides large set of data from recording of net pen, relevant to develop and test methods for optimal and efficient inspection operations in net pens. This means that it is expected that both the research community and the aquaculture industry will benefit greatly from the utilization of the SALAQUA dataset.

VI. ACKNOWLEDGEMENTS

The authors express their sincerest gratitude to Kay Arne Skarpenes and Terje Bremvåg who assisted during the field trials. The work was funded by the Research Council of Norway through projects Resifarm (no. 327292) and CHANGE (no. 313737), and by SINTEF Ocean.

REFERENCES

- [1] M. Føre, K. Frank, T. Norton, E. Svendsen, J. A. Alfredsen, T. Dempster, H. Eguiraun, W. Watson, A. Stahl, L. M. Sunde, *et al.*, “Precision

- fish farming: A new framework to improve production in aquaculture,” *biosystems engineering*, vol. 173, pp. 176–193, 2018.
- [2] E. Kelasidi and E. Svendsen, “Robotics for sea-based fish farming,” in *Encyclopedia of Smart Agriculture Technologies*, pp. 1–20, Springer, 2023.
- [3] H. B. Amundsen, M. Xanthidis, M. Føre, S. J. Ohrem, and E. Kelasidi, “Aquaculture field robotics: Applications, lessons learned and future prospects,” *arXiv preprint arXiv:2404.12995*, 2024.
- [4] P. Rundtop and K. Frank, “Experimental evaluation of hydroacoustic instruments for ROV navigation along aquaculture net pens,” *Aquacultural Engineering*, vol. 74, pp. 143–156, 2016.
- [5] H. B. Amundsen, W. Caharija, and K. Y. Pettersen, “Autonomous ROV inspections of aquaculture net pens using DVL,” *IEEE Journal of Oceanic Engineering*, vol. 47, no. 1, pp. 1–19, 2021.
- [6] S. J. Ohrem, L. D. Evjemo, B. O. A. Haugaløkken, H. B. Amundsen, and E. Kelasidi, “Adaptive speed control of ROVs with experimental results from an aquaculture net pen inspection operation,” in *2023 31st Mediterranean Conference on Control and Automation (MED)*, pp. 868–875, IEEE, 2023.
- [7] S. J. Ohrem, B. O. A. Haugaløkken, and C. Holden, “Application of modified model reference adaptive controller and observer (mraco) for speed control of an unmanned underwater vehicle,” in *2024 15th IFAC Conference on Control Applications in Marine Systems, Robotics and Vehicles*, p. Accepted for publication, IEEE, 2024.
- [8] B. O. Haugaløkken, H. B. Amundsen, H. S. Fadum, J. T. Gravidahl, and S. J. Ohrem, “Adaptive generalized super-twisting tracking control of an underwater vehicle,” in *2023 IEEE Conference on Control Technology and Applications (CCTA)*, pp. 687–693, IEEE, 2023.
- [9] B. O. Haugaløkken, O. Nissen, M. B. Skaldebø, S. J. Ohrem, and E. Kelasidi, “Low-cost sensor technologies for underwater vehicle navigation in aquaculture net pens,” *IFAC-PapersOnLine*, vol. 58, no. 20, pp. 87–94, 2024.
- [10] W. Akram, A. Casavola, N. Kapetanović, and N. Miškovic, “A visual servoing scheme for autonomous aquaculture net pens inspection using rovs,” *Sensors*, vol. 22, no. 9, p. 3525, 2022.
- [11] C. Schellewald, A. Stahl, and E. Kelasidi, “Vision-based pose estimation for autonomous operations in aquacultural fish farms,” *IFAC-PapersOnLine*, vol. 54, no. 16, pp. 438–443, 2021.
- [12] D. Botta, L. Ebner, A. Studer, V. Reijgwart, R. Siegwart, and E. Kelasidi, “Framework for robust localization of uavs and mapping of net pens,” *arXiv preprint arXiv:2409.15475*, 2024.
- [13] S. J. Ohrem, B. O. A. Haugaløkken, and C. Holden, “Application of modified model reference adaptive controller and observer (mraco) for speed control of an unmanned underwater vehicle,” *IFAC-PapersOnLine*, vol. 58, no. 20, pp. 196–202, 2024.